Electronic Supporting Information

Solvent-free dynamic nuclear polarization enhancements in organically modified mesoporous silica

Marcos de Oliveira, Jr.,[a,b,†,*] Kevin Herr,[a,†] Martin Brodrecht,[a] Nadia B. Haro-Mares,[a] Till Wissel,[a] Vytautas Klimavicius,[a,c] Hergen Breitzke,[a] Torsten Gutmann,[a] Gerd Buntkowsky [a,*]

a. *Institut für Physikalische Chemie, Technische Universität Darmstadt, 64287 Darmstadt, Germany*
b. *São Carlos Institute of Physics, University of São Paulo, PO Box 369, 13560-970, São Carlos, SP, Brazil*
c. *Institute of Chemical Physics, Vilnius University, Sauletekio av. 3, LT-10257 Vilnius, Lithuania*

† Equally contributing authors

* Corresponding authors.

Table S1 – Weights of Fmoc-Gly-OH and 3-Carboxy-PROXYL precursors used in the synthesis. The overall mass of the final materials (yield mass) is also given.

Sample	Weigh Fmoc-Gly-OH [mg]	Weigh 3-Carboxy-PROXYL [mg]	Yield [mg]
99.5Fmoc/0.5Prx	79	0.3	54
95Fmoc/5Prx	75	2.5	59
90Fmoc/10Prx	71	5	58
75Fmoc/25Prx	59	12	50
50Fmoc/50Prx	40	25	64

Table S2: Median pore diameters calculated by the BJH (left) and NLDFT (right) method of the prepared SBA-15 with APTES linker and functionalized mesoporous silica materials as obtained from BET analysis.

Sample	Pore diameter by BJH / nm	Pore diameter by NLDFT / nm
SBA-15 with APTES	5.5	7.9
99.5Fmoc/0.5Prx	5.3	6.6
95Fmoc/5Prx	5.3	7.0
90Fmoc/10Prx	5.4	6.6
75Fmoc/25Prx	5.3	6.6
50Fmoc/50Prx	5.2	6.6

Table S3. Pore volume (Gurvich at p/p^0 0.95), specific surface area (BET), nitrogen loading and carbon/nitrogen ratio of the support material determined by EA.

Sample	Pore Volume (BET) / $cm^3 \cdot g^{-1}$	Surface Area (BET) / $m^2 \cdot g^{-1}$	Nitrogen loading (EA) / $mmol \cdot g^{-1}$	C/N ratio (Theo.)	C/N ratio (Exp.)
SBA-15 with APTES	0.72	537	1.78 ± 0.3	3.00	3.13 ± 0.5

Table S4 - Elemental Analysis. Two measurements were performed for each sample.

Sample	C/N ratio	Carbon (%)	Hydrogen (%)	Nitrogen (%)
Amine functionalized SBA-15	2.835	8.018	3.11	2.829
Amine functionalized SBA-15	2.842	7.728	3.399	2.719
X 0.5	3.611	17.24	3.013	4.775
X 0.5	3.65	17.1	2.859	4.685
X 5	3.408	17.05	3.271	5.004
X 5	3.29	16.71	3.682	5.079
X 10	3.68	16.59	3.101	4.509
X 10	3.511	16.39	3.108	4.667
X 25	3.092	15.48	3.291	5.006
X 25	3.112	15.43	3.349	4.958
X 50	3.266	15.51	3.024	4.747
X 50	3.268	14.96	3.182	4.578

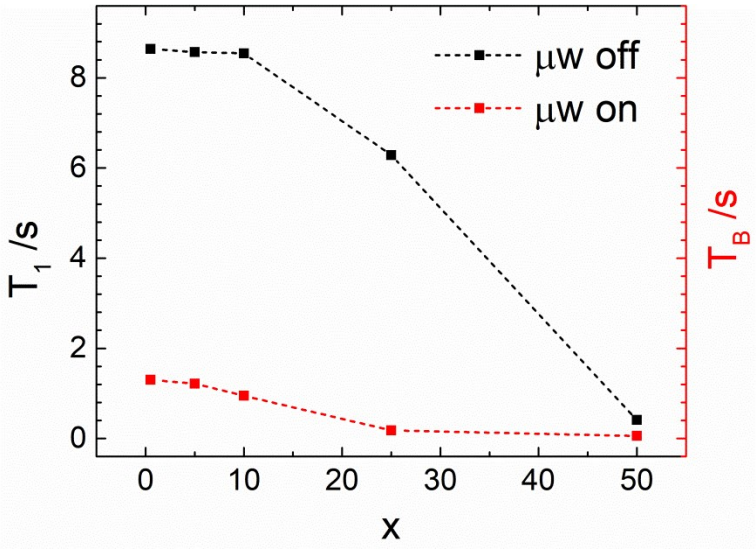

Figure S1 – ^1H spin-latice relaxation times (T_1, µw off) and DNP build-up times (T_B, µw on) as a function of composition parameter *x* for the investigated samples. Values were obtained from unconstrained least-square fittings of saturation-recovery curves by using stretched exponential functions.

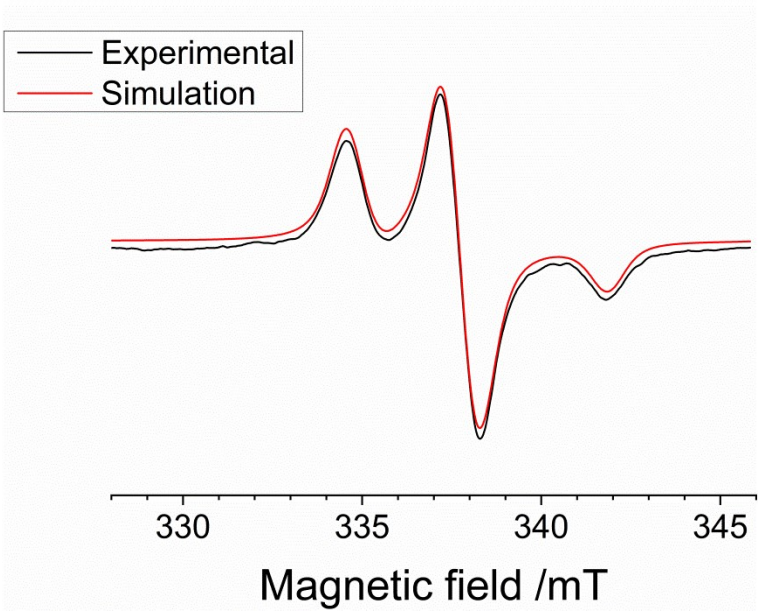

Figure S2 – Experimental (black curve, bottom) and simulated (red curve, top) cw EPR spectra for the sample with x = 10 mol%. The experimental spectrum was measured at 100 K. The simulation was performed using the EasySpin[1] package for the Matlab® software. The simulation uses the "pepper" function from EasySpin,[1] which considers a solid state powder. The system consists of an electron spin with rhombic g and ^{14}N-hyperfine tensors (^{15}N was also considered in natural abundance). The parameters were optimized by comparing experimental and simulated spectra, using a combination of least-square fitting and genetic algorithms and taking the parameters reported by Dhanasekaran at al.[2] as initial guess. The final parameters for the simulation are g_{xx} = 2.0088, g_{yy} = 2.0057, g_{zz} = 2.0021, A_{xx} = 12 ± 1 MHz and A_{yy} = 14 ± 1 MHz and A_{zz} = 102 ± 1 MHz. The simulation also considers a Gauss-Lorentz (0.6-0.4) isotropic line broadening of 28 MHz (peak-to-peak).

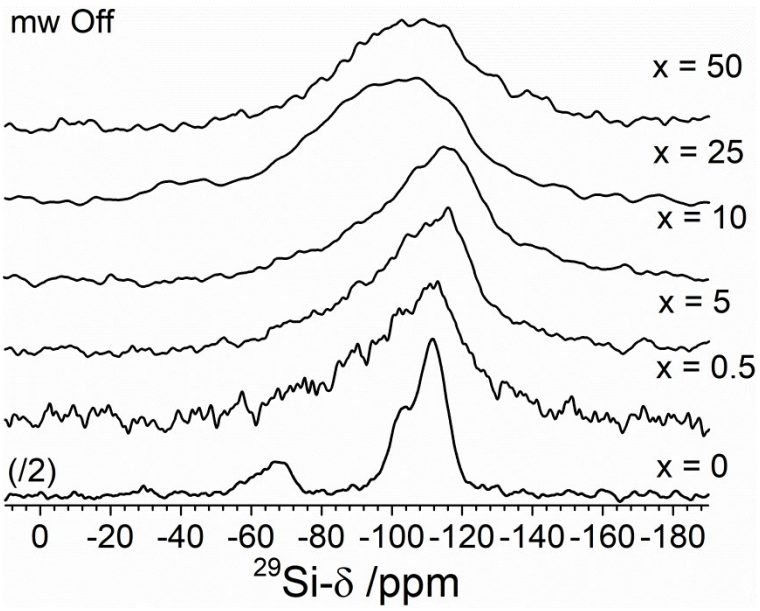

Figure S3 – ^{29}Si MAS NMR spectra for the investigated samples (x = 0.5 to 50) and for a sample without carboxy-PROXYL radical (x = 0). The spectral line width increases for increasing radical concentration due to electron-nucleus hyperfine interaction.

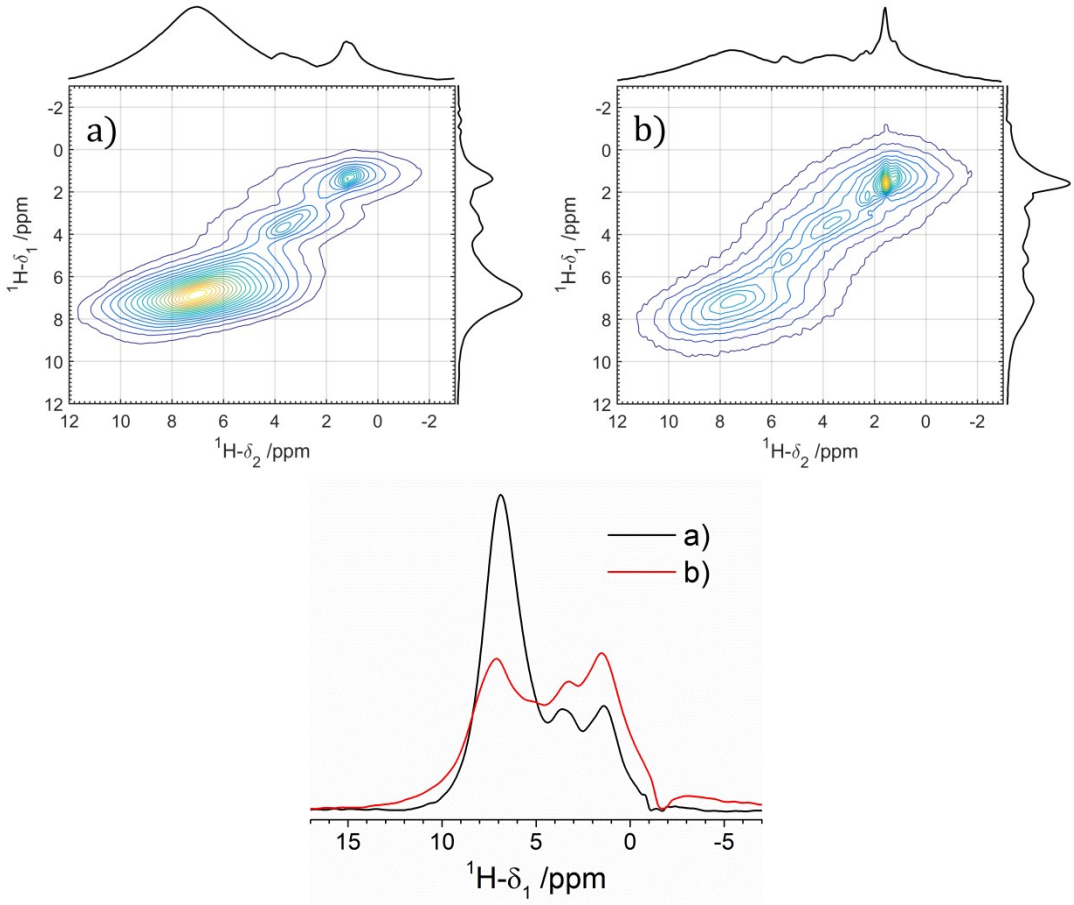

Figure S4 – Top: ^{1}H–^{1}H MAS FSLG spectrum of a) mesoporous SBA-15 functionalized with APTES and Fmoc-Glycine (diamagnetic sample) and b) mesoporous SBA-15 functionalized with APTES, Fmoc-Glycine and Carboxy-PROXYL radicals (paramagnetic sample, *x* = 50). Skyline projections are also displayed. Bottom: comparison of the projections taken from the sum over the indirectly detected (δ_1) dimension for both spectra shown on top. 2D spectra were measured with a z-filtered ^{1}H-^{1}H correlation pulse sequence with Frequency Switched Lee–Goldberg decoupling during t_1 evolution.[3] The experiments were performed using ^{1}H carrier frequency of 400 MHz, spinning rate of 10 kHz and z-filter delay of 1 μs. In this experiment a MAS spectrum is detected in the direct domain (δ_2) while FSLG decoupled signal is achieved in the indirect domain (δ_1). Due to the FSLG decoupling the ^{1}H-^{1}H dipolar coupling is averaged out and the line broadening caused by ^{1}H spin-spin relaxation mechanism is suppressed. The result is a resolution enhancement in the δ1 projection and the detection of the δ2 projections similar to the 1D spectrum. On the other hand, the electron-nucleus hyperfine interaction is not averaged out by FSLG decoupling leading to fast relaxation of areas containing the radicals. As a result, only components outside of the effective paramagnetic shell will survive seen as relative enhancement of the peak at 1.2 ppm in the projections, accompanied by a higher resolved δ_1 projections. This peak belongs most probably to mobile and isolated water molecules on the surface,[4] far away from the radicals.

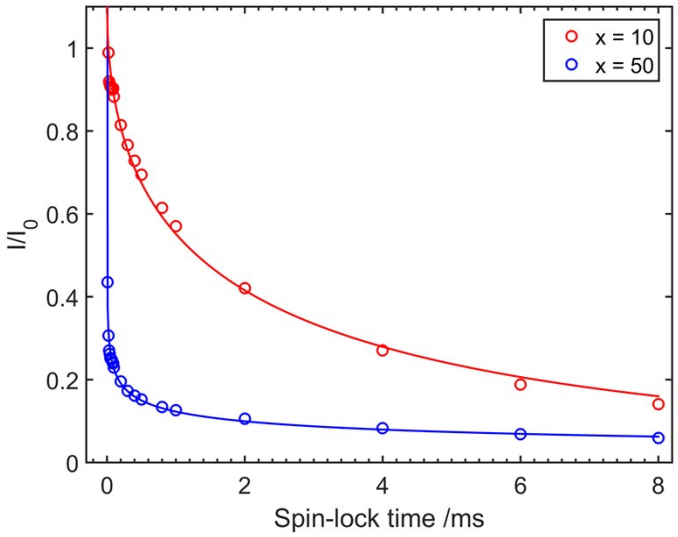

Figure S5 – ^{1}H magnetization as a function of the spin-lock time for samples x = 10 and x = 50, measured using a 90º-spinlock pulse sequence, nuclei are excited by a 90º pulse and then spin-locked by a continuous wave pulse (with a phase shift of $\pi/2$ relative to the excitation pulse) for a time τ.[5] The experimental points are normalized to the extrapolated equilibrium magnetization. The evolution of the magnetization curves gives information about the ^{1}H spin lattice relaxation in the rotating frame ($T_1\rho$). Solid curves are exponential fit to the data, using a stretched exponential function of the form $I = I_0 \exp\left(-\left(t/T_1^{\rho}\right)^{\beta}\right)$ (see parameter values in Table S5). Due to the distribution of distances between H species and the unpaired electrons in the sample, a continuous distribution of relaxation times is expected. Clearly, for the sample with x = 50 the effective ^{1}H spin relaxation is much faster than for the sample with x =10. For this reason, ^{1}H-^{13}C CP transfer could not be achieved for sample x = 50 (see main text).

Table S5: Fitting parameters to a stretched exponential decay function, $I = I_0 \exp\left(-\left(t/T_1^{\rho}\right)^{\beta}\right)$, adjusted on the data shown in Figure S5.

Sample	$T_1\rho$ (ms)	β
x = 10	2.1	0.5
x = 50	2×10^{-3}	0.1

References

1 S. Stoll and A. Schweiger, EasySpin, a comprehensive software package for spectral simulation and analysis in EPR, *J. Magn. Reson.*, 2006, **178**, 42–55.

2 A. Dhanasekaran, S. Kotamraju, C. Karunakaran, S. V. Kalivendi, S. Thomas, J. Joseph and

B. Kalyanaraman, Mitochondria superoxide dismutase mimetic inhibits peroxide-induced oxidative damage and apoptosis: Role of mitochondrial superoxide, *Free Radic. Biol. Med.*, 2005, **39**, 567–583.

3 B. Kumari, M. Brodrecht, T. Gutmann, H. Breitzke and G. Buntkowsky, Efficient Referencing of FSLG CPMAS HETCOR Spectra Using 2D 1H–1H MAS FSLG, *Appl. Magn. Reson.*, 2019, **50**, 1399–1407.

4 B. Grünberg, T. Emmler, E. Gedat, I. Shenderovich, G. H. Findenegg, H.-H. Limbach and G. Buntkowsky, Hydrogen Bonding of Water Confined in Mesoporous Silica MCM-41 and SBA-15 Studied by ^{1}H Solid-State NMR, *Chem. - A Eur. J.*, 2004, **10**, 5689–5696.

5 A. Abragam, *The Principles of Nuclear Magnetism*, Oxford Univ. Press, Oxford, 1961.